Saudi Journal of Biological Sciences 29 (2022) 18–29

Contents lists available at ScienceDirect

Saudi Journal of Biological Sciences

journal homepage: www.sciencedirect.com

Original article

In silico identification of potential inhibitors against main protease of SARS-CoV-2 6LU7 from *Andrographis panniculata* via molecular docking, binding energy calculations and molecular dynamics simulation studies

Mayakrishnan Vijayakumar [a,1], Balakarthikeyan Janani [b,1], Priya Kannappan [b,*], Senthil Renganathan [c,d], Sameer Al-Ghamdi [e], Mohammed Alsaidan [f], Mohamed A. Abdelaziz [g,h], Abubucker Peer Mohideen [g], Mohammad Shahid [g], Thiyagarajan Ramesh [g,*]

[a] *Laboratory of Cell and Molecular Biology, Grassland and Forage Science Division, National Institute of Animal Science, Rural Development Administration, Cheonan-si, Chungcheongnam-do 31000, Republic of Korea*
[b] *Department of Biochemistry, PSG College of Arts and Science (Autonomous), Affiliated to Bharathiar University, Coimbatore 641014, Tamil Nadu, India*
[c] *Department of Bioinformatics, Marudupandiyar College, Thanjavur 613 403, Tamil Nadu, India*
[d] *Lysine Biotech Private Limited, Periyar Technology Incubator, DST Business Incubator, Periyar Maniammai Institute of Science and Technology (PMIST), Vallam, Thanjavur 613403, Tamil Nadu, India*
[e] *Family and Community Medicine Department, College of Medicine, Prince Sattam Bin Abdulaziz University, Al-Kharj 11942, Kingdom of Saudi Arabia*
[f] *Internal Medicine Department, College of Medicine, Prince Sattam Bin Abdulaziz University, Al-Kharj 11942, Kingdom of Saudi Arabia*
[g] *Department of Basic Medical Sciences, College of Medicine, Prince Sattam Bin Abdulaziz University, Al-Kharj 11942, Kingdom of Saudi Arabia*
[h] *Department of Medical Physiology, College of Medicine, Al-Azhar University, Cairo, Egypt*

ARTICLE INFO

Article history:
Received 18 September 2021
Revised 12 October 2021
Accepted 21 October 2021
Available online 29 October 2021

Keywords:
Corona
SARS-CoV-2
COVID-19 (6LU7)
Natural compounds
Diterpenoids
Andrographolide
Molecular dynamic simulations

ABSTRACT

Background: The ongoing global outbreak of new corona virus (SARS-CoV-2) has been recognized as global public health concern since it causes high morbidity and mortality every day. Due to the rapid spreading and re-emerging, we need to find a potent drug against SARS-CoV-2. Synthetic drugs, such as hydroxychloroquine, remdisivir have paid more attention and the effects of these drugs are still under investigation, due to their severe side effects. Therefore, the aim of the present study was performed to identify the potential inhibitor against main protease SARS-CoV-2 6LU7.
Objective: In this study, RO5, ADME properties, molecular dynamic simulations and free binding energy prediction were mainly investigated.
Results: The molecular docking study findings revealed that andrographolide had higher binding affinity among the selected natural diterpenoids compared to co-crystal native ligand inhibitor N3. The persistent inhibition of Ki for diterpenoids was analogous. Furthermore, the simulations of molecular dynamics and free binding energy findings have shown that andrographolide possesses a large amount of dynamic properties such as stability, flexibility and binding energy.
Conclusion: In conclusion, findings of the current study suggest that selected diterpenoids were predicted to be the significant phytonutrient-based inhibitor against SARS-CoV-2 6LU7 (M^{pro}). However, preclinical and clinical trials are needed for the further scientific validation before use.

1. Introduction

The novel corona virus (SARS-CoV-2) that emerged at the end of year 2019, is considered as global public health concern, since it causes high morbidity and mortality (Cui et al., 2019; Arasu et al., 2020). This human pathogenic new virus was first found in Wuhan city, China, where an unspecified cause of pneumonia was reported last year in December 2019 (Gil et al., 2020). Similarly, SARS-CoV (severe acute respiratory syndrome corona virus) and MERS-CoV (Middle East respiratory syndrome-corona virus), new COVID-19 virus also belongs to the family of Coronaviridae

Abbreviations: ACE 2, Angiotensin Converting Enzyme; CNS, central nervous system; COVID-19, coronavirus disease 2019; M^{pro}, Main protease; SARS-CoV-2, Severe acute respiratory syndrome coronavirus 2.

* Corresponding authors.
E-mail addresses: priyak08@gmail.com (P. Kannappan), thiyagaramesh@gmail.com (T. Ramesh).

[1] These authors contributed equally to this work.

Peer review under responsibility of King Saud University.

Production and hosting by Elsevier

https://doi.org/10.1016/j.sjbs.2021.10.060
1319-562X/

(Gil et al., 2020). It is assumed that COVID-19 virus originated from bats and with the help of others sources transmitted to humans (Ghosh et al., 2021). This COVID-19 virus belongs to the class of RNA virus, which is made up of 22–26 kilo base. Four structural proteins such as spike, nucleocapsid, membrane and envelop are encoded by the genome of this positive sensed RNA virus (Wahedi et al., 2021). The COVID-19 virus is believed to be spread by physical contact with infected individuals, secretions from the respiratory system, and through air droplets, they also have the potency to remain active on the contact surface for several days (Shetty et al., 2020). Individual affected by this virus, develop symptoms like breathing difficulty, fever, cough, abdominal pain, and nausea. Conditions like pneumonia severe acute respiratory syndrome, renal failure, and death due to multiple organ failure appear in severe infected cases (Wang et al., 2020). The individual infected from respiratory problems which are caused due to the binding of the virus to angiotensin-converting enzymes (ACE2) which is found in alveoli of the lungs and regulates the cells functions. COVID-19 virus binding to ACE2 leads to the discharge of the RNA into the cells, then the RNA starts its translation process, during this process polyproteins are necessary for the virus are made, proteolysis of the polyproteins occurs to provide active constituents. An enzyme named RNA polymerase plays an important role in the RNA multiplications which binds to the active constituents in order to produce a novel virus particle that infects the neighbor cells. Once, there is an increased infected cells, there is increased liquid secretion in alveoli that make problems in respiration (Kumar et al., 2021).

Some potential targets are spike protein, RNA dependent RNA polymerase, ACE2 and viral protease (Liu et al., 2020; Ghosh et al., 2021). The genome of novel COVID-19 virus encodes two major polyproteins such as pp1a and pp1ab which are similar to most of the Coronaviridae-genome. The two protease (papain-like protease) and 3CL protease (3C like protease) are encoded by ORF1a/b; it plays an important role in cleaving and transforming the two polyproteins into active and mature non-structural protein (Gil et al., 2020). By considering the role played by proteases in viral replication and host cell response regulation, particularly, the crystallized the M^{pro} of COVID-19 (PDB id: 6LU7) from the SARS-CoV that provide the opportunity to control the disease by demonstrating as a drug target (Liu et al., 2020). Therefore, they should be considered as key targets for developing antiviral drugs. In human history and evolution, natural products play a significant role in the development of drugs for the treatment of various diseases. Plant and animal derived molecules are considered as essential sources of bioactive molecules. Bioactive molecules from plants have been widely used in various field including pharmaceutical and medicine, particularly for the treatment of inflammation, cancer, oxidative stress, viral infections and etc., Several antiviral molecules from plants have already been described by the activity against Dengue virus, Enterovirus, Hepatitis B, Influence virus and HIV (Lin et al., 2014; Hussain et al., 2017; Lee and Hur, 2017; Denaro et al., 2020; Ahmed et al., 2020).

Andrographis panniculata (*A. panniculata*) is a medicinal herb native to India although used in many countries of Southeast Asia (Chao and Lin, 2010). The extremely bitter taste nature of *A. panniculata* have been used to treat various diseases including, liver disorders, bowel problems in children, colic pain, common cold, and infection of the upper respiratory tract and also it possess immunostimulant, antidiarrheal, anti-inflammatory, antibacterial, antimalarial activities. The presence of diverse phyto-molecules like labdane, diterpenoids lactones, flavonoids and some miscellaneous compounds were also reported by the phytochemical studies (Mishra et al., 2009). About 4% of the whole plant comprises andrographolide, neoandrographolide, 14-deoxyandrographile, 14-deoxy-11, 12-didehydroandrographolide and, andrographanin are other diterpene compounds present in the aerial parts of the plant (Okhuarobo et al., 2014). Previous study confirmed that *A. panniculata* had antiviral potential against human immune deficiency virus (HIV), also one of diterpenoids compounds possess antiviral potential against HIV, human simplex virus (HSV), flaviviruses, pestiviruses and (epstein-bar virus) EBV (Jayakumar et al., 2013). With the above considerations, the aim of the present study was designing to develop a promising protease inhibitor against M^{pro} of COVID-19 by the screening of five majorly present diterpenoids molecules of andrographolide, neoandrographolide, 14-deoxyandrographolide, 14-deoxy-11, 12-didehydroandrographolide and andrograpanin from *A. panniculata*. Also, we have investigated whether these are satisfying Lipinski's Rule of Five (RO5) and ADME properties. Finally, these compounds were confirmed with molecular docking and dynamic simulation.

2. Materials and methods

2.1. Preparation of ligands

The structure of ligands in sdf format was retrieved using PubChem (https://pubchem.ncbi.nlm.nih.gov). PubChem is an archive of chemical compounds and biological activities comprising 3 databases, which is including substance, compound and bioassay databases (Salehi et al., 2020). The ligands and their compound CID were andrographolide (CID: 5318517), andrograpanin (CID: 11666871), neoandrographolide (CID: 9848024), 14-deoxyandrographolide (CID: 11624161) and, 14-deoxy, 11,12-didehydroandrographolide (CID: 5708351). The ligands were converted in to pdb format using Pymol software, then the ligands were prepared using AutoDock tools to obtain pdbqt file format of ligands (Ghosh et al., 2021). Drug-likeliness of the ligands were determined using RO5 which proposes molecular characteristics like molecular weight not>500 Da, ClogP < 5, hydrogen bond donor < 5, hydrogen acceptors < 5, shows good permeation and oral absorption. RO5 of the ligands was calculated using the Supercomputing Facility of Bioinformatics & Computational Biology (http://www.scfbio-iitd.res.in/software/drugdesign/lipinski.jsp), Indian Institute of Technology (IIT), Delhi, India.

2.2. Preparation of protein

The 3D protein structure of COVID-19 M^{pro} with co crystallized ligand structure (PDB ID: 6LU7) was obtained from protein data bank (https://www.rcsb.org) in pdb format. PDB is a worldwide protein data bank that has 3D structural data of the large proteins (Rosidi et al., 2016). The protease consists of two chains A and C, chain A belongs to protease and chain C belongs to N3 inhibitor N-[(5methylisoxazol-3yl) carbonyl] alanyl-L-valyl-N-1- (1R,2Z)-4-(benzyloxy)-4-oxo-1–1- [(3R)-2-oxopyprolidin-3-3yl] methyl but-2-enyl)-L-lucinamide. The protein structure was prepared by removing co-crystallized ligand and water molecules, polar hydrogens and charges were added using AutoDock tools. Finally, pdbqt file format of the protease was obtained.

2.3. ADMET properties

The pharmacokinetic properties including polar surface area and AlogP were observed using SWISS ADME (http://www.swissadme.ch/) an online web-server. pkCSM ADMET web-server was used to determine the absorption, distribution, metabolism, excretion, and toxicity of the ligands (Han et al., 2019). $CaCO_2$ permeability, intestinal absorption, skin permeability, substrate or inhibitor of P-glycoproteins was used to measure the absorption characteristics of drugs. The drug distribution depends on blood

brain barrier (BBB) permeability, central nervous system (CNS) permeability and volume distribution (VDs). Cytochrome P450 model used for substrate CYP2D6 and CYP3A4, inhibitor CYP1A2, CYP2C19, CYP2C9, CYP2D6 and CYP3A4 used to determine the metabolism of drugs. The total clearance model and renal OCT2 substrate was used to depict the excretion of drug.

2.4. Molecular docking

Molecular docking was performed using AutoDock version 4.2 which is supported by tools like AutoDock tools, MGL tools and Rasmol. The native ligand N3 was chosen to find binding affinity. The position of native ligand N3 in the M^{pro} on the binding site was determined by using Autogrid and with the help of XYZ coordinates (-14.649, 11.549 and 70.535 respectively). The same grid coordinates and grid box (404040) were used for all the ligands. Genetic Algorithm parameters were then used to perform docking by using 10 runs of Genetic Algorithm docking. The estimated free energy of binding of all the selected molecules was observed for 10 runs. Among the docked factors confirmation with lowest RMSD (root mean square deviation) values was selected and analysed by using AutoDock 4.2, Pymol 4.50 and Biovia discovery studio.

2.5. Molecular dynamics simulation

Main protease of SARS-COVID-19 was selected as the target for virus progression and pathway. Molecular dynamics simulation was executed for recording the frames of protein–ligand complex during molecular recognition and association. The receptor and ligand topology files were prepared by Groningen Machine for Chemical Simulations (Gromacs 2020.1 version) and PRODRG1 server. The Force Field GROMOS96 43a1 was applied to all the complex system and (SPC) single point charge water model was preferred, respectively. Cubic box was adjusted to main protease-inhibitors complex and solvated accordingly. Counter ions were added to neutralize system that was of sodium (NA) and chloride (CL). Energy minimization of complex system was executed with steps 50,000 and maximum force < 10.0 kJ/mol by steepest descent minimization algorithm. The NVT (Number of particles, volume and temperature) and NPT (Number of particles, pressure and temperature) ensemble analysis were observed for 100 (ps) picoseconds with leap-frog integrator method. Alpha-carbon atoms were allowed to move flexibly to ensure the system equilibration. Position restraints and bond forming were observed by linear constraint solver algorithm. Calculation of electrostatic interaction was obtained by Particle Mesh Ewald for long-range electrostatics (PME) with the cut of value (1.2 nm) and grid spacing (0.16). The equilibrated system was further imported to simulation for the production with temperature (300) and pressure (1 atm) by modified berendsen thermostat. The molecular dynamics production were analyzed for 50 ns and frames recorded for every 2 fs. Trajectories obtained from the molecular dynamics production were used to prepare root mean square deviation, root mean square fluctuation and hydrogen bonding.

3. Results

3.1. Analysis of ligand characteristics

In this experiment, first our focus was to check each molecule against M^{pro} of COVID-19, whether it met the RO5 such as chemical formula, structure, and properties that define RO5 and were presented in Table 1 and 2. Results of the current study demonstrated that the selected all five ligands found to adapt the RO5 without incurring any violation of the RO5, while native ligand N3 incurred two violations. Based on the RO5 rules they can be selected as the drug candidate against M^{pro} of COVID-19.

3.2. Analysis of ADME characteristics of ligand

Further we examined the ADME pharmacokinetics, absorption, distribution, excretion and toxicity of selected bioactive compounds by using Swiss ADME and admetSAR server and the findings were shown in Table 3. The polar surface area of all the diterpenoids except neoandrographolide was found to be < 100, which implies that the diterpenoids except neoandrographolide had greater membrane permeability or oral absorption. Also, the study results revealed that the selected bioactive molecules showed the Papp Coefficient value to be > $8x10^{-6}$, this indicates that the selected molecules are easy to absorb due to its high permeability property. Among the selected compounds, andrograpanin had greater intestinal absorption (100%), and neoandrographolide had lower intestinal absorption (499.25%). Skin permeability of a compound is expressed in Log Kp value, if the value of Log Kp is greater than −2.5 (Log Kp > 2.5) then the compound is found to have low skin permeability. The five diterpenoids were predicted to have low skin permeability because all the compounds have Log Kp > −2.5. The Blood-Brain Barrier (BBB) permeability is a parameter used to measure whether the drug candidate can pass through the Blood-Brain Barrier or not. This BBB permeability is measured in terms of LogBB, if the value of LogBB $\geq$ 0.3 then the compound is said to have good BBB permeability, LogBB between 0.3 and −1, the compounds can still pass-through BBB, LogBB < −1, the compounds relatively have poor BBB permeability (Kunwittaya et al., 2013). Among the results, Andrographolide, Andrograpanin, 14- Deoxyandrographolide, and 14- deoxy,11,12-didehydroandrographolide found to have LogBB value between 0.3 and −1, so these four diterpenoids were predicted to cross BBB, for Neoandrographolide LogBB value is less than −1, hence it is found to have relatively poor BBB permeability.

3.3. Molecular docking and dynamics simulation analysis

Table 4 comprises of ligand names, their docked structure (Fig. 1) with protease, their corresponding energy and their constant Ki value. Among the selected compounds andrographolide showed the highest binding energy −8.09 Kcal/mol, followed by 14-deoxy,11,12-deoxyandrographolide with binding energy −7.92 Kcal/mol, neoandrographolide with binding energy −7.76 Kcal/mol, 14-deoxyandrographolide with binding energy −7.67 Kcal/mol. The binding energy of N3 (crystallized ligand) was found to be −7.69 Kcal/mol. The inhibition constant Ki for andrograpanin was 1.18 μM, for neoandrographolide was 2.59 μM, for 14-deoxyandrographolide was 2.05 μM, and for 14-deoxy,11,12-deox yandrographolide was 1.57 μM. The 2D and 3D visualization of molecular interaction analysis between M^{pro} of COVID-19 with selected compounds are showed in Figs. 2 and 3. The nature of the bond, amino acid residue involved and their bond distance is given in Table 4. The native ligand N3 made a total of four hydrogen bonds with interacting amino acid residues Gly143, Ser114, His164, and Glu166 with a bond distance of 1.56, 2.50, 3.07 and 2.58 Å, respectively. Andrographolide made two hydrogen bonds with M^{pro} by interacting with amino acids Phe140 and Ser144 with a bond distance of 2.07 and 1.90 respectively. Andrographanin made two hydrogen bonds with M^{pro} by interacting with amino acids His41 and Asn142 with a bond distance of 2.94 and 2.13 Å, respectively. Neoandrographolide made six hydrogen bonds with M^{pro} by interacting with amino acids Cys145, Met165, Glu166, Arg188, and Glu189 with a bond distance of 2.62, 2.74, 2.17, 1.96, 2.07, and 2.20 Å respectively. 14-deoxyandrographolide made three hydrogen bonds with M^{pro} by interacting with amino acids

Table 1
List of selected bioactive compounds from *A. panniculata* for potential antiviral activity against M^{pro} of COVID-19.

Name of compound	Molecular formula	Structure	Pharmacological activity
N3	$C_{35}H_{48}N_6O_8$	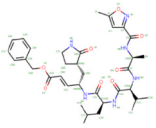	–
Andrographolide	$C_{20}H_{30}O_5$	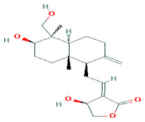	Anticancer, anti-diabetic, anti-inflammatory, antibacterial, anti-malarial, anti-hepatitis, anti-HIV, anti-atherosclerosis and hepatoprotective
Andrograpanin	$C_{20}H_{30}O_3$	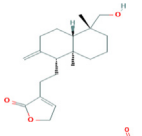	Anti-biofilm, anti-HIV,
Neoandrographolide	$C_{26}H_{40}O_8$	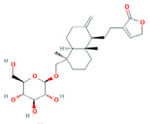	Anti-inflammatory, anti-malarial, immunomodulatory
14-Deoxyandrographolide	$C_{20}H_{30}O_4$	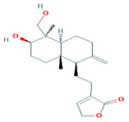	Anticancer, anti-inflammatory, anti-HIV
14-deoxy-11,12-didehydroandropholide	$C_{20}H_{28}O_4$	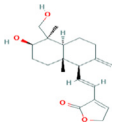	Anti-cancer, anti-HIV, anti-atherosclerosis, relaxant, anti-hyperglycemic

Table 2
Lipinski's rule of five (RO5) of M^{pro} of COVID-19 and selected bioactive compounds from *A. panniculata* for protein potential inhibitors.

Ligands	Molecular formula	Molecular weight <500	LogP <5	H-bond donor < 5	H-bond acceptor < 10	Violations	Meet RO5 criteria
N3	$C_{35}H_{48}N_6O_8$	680.00	0.6967	5	12	+	–
Andrographolide	$C_{20}H_{30}O_5$	332.00	3.1153	2	4	–	+
Andrograpanin	$C_{20}H_{30}O_3$	318.00	4.0209	1	3	–	+
Neoandrographolide	$C_{26}H_{40}O_8$	480.00	1.8452	4	8	–	+
14-Deoxyandrographolide	$C_{20}H_{30}O_4$	334.00	2.9917	2	4	–	+
14-deoxy-11,12-didehydroandropholide	$C_{20}H_{28}O_4$	332.00	2.7677	2	4	–	+

His41 and Leu141 with a bond distance of 2.99, 2.00 and 2.17 Å, respectively. Likewise, 14-deoxy,11,12-deoxyandrographolide made four hydrogen bonds with M^{pro} by interacting with amino acids His41, Tyr54, Leu141, and Ser144 with a bond distance of 2.82, 2.09, 1.98 and 2.25 Å, respectively. Similarly, all of selected bioactive compounds also bind with these two catalytic residues (His41 and Cys145) when both the hydrogen and non-hydrogen bonds were considered. Also, apart from andrographolide other selected bioactive compounds have also demonstrated a significant binding energy towards M^{pro} of COVID-19.

Main protease with andrographolide derivatives were analyzed for conformational changes and constraints. Trajectories recorded for 50 nano seconds were chosen to evaluate the ligand position during a longer simulation by root mean square deviation, fluctuation and hydrogen bonding. From the result of RMSD (Fig. 4), RMSF (Fig. 5) and hydrogen bonding plots (Fig. 6), it is observed that main protease – andrographolide derivatives are strong enough to maintain stability. All the diterpenoids differed in physicochemical properties were sharing the free energy of binding between −5 to −8 kcal/mol. In total, binding energies have been calculated and considered for better interaction that are reasonable for andrographolide (-7.06 kcal/mol) and 14-deoxyandrographolide (−7.01 kcal/mol). 14-deoxy-11,12-didehydroandropholide (−6.96 kcal/mol) and andrographonin (−6.87 kcal/mol) are recorded for energy differences while neoandrographolide is found with −5.47 kcal/mol.

4. Discussion

The novel coronavirus causes massive public health crisis in all over the world. Since there are no approved drugs or vaccines available, new treatment strategies are urgently needed for treating COVID-19 (Kumar et al., 2020; Bhojaraj et al., 2021). Computational biology based drug development model are enabling the identification of new drugs and used to be aware of molecular aspects of protein targets and target-ligand interactions (Sheikh et al., 2020). Repurposing of FDA approved naturally identified antiviral drugs will be the right choice at this time for discovering

Table 3
Pharmacokinetics, absorption, distribution, excretion and toxicity of selected bioactive compounds from *A. panniculata* determined by using SWISS ADME and pkCSM ADMET web server.

Parameters	N3	Andrographolide	Andrograpanin	Neoandrographolide	14-deoxyandrographolide	14-deoxy11,12-didehydro andrographolide
PSA	197.83	86.99	46.53	125.68	66.76	66.76
AlogP98	2.74	2.33	3.95	2.33	3.15	2.52
Absorption						
Water solubility	−4.181	−3.384	−4.199	−3.826	−3.296	−3.203
CaCo2 permeability	0.501	1.24	1.444	0.502	1.236	1.253
Intestinal absorption	63.398	98.427	100	49.295	98.713	99.561
Skin permeability	−2.736	−3.119	−3.13	−2.747	−3.106	−3.117
P-glycoprotein substrate	+	+	+	+	+	+
P-glycoprotein-I inhibitor	+	+	+	+	+	+
P-glycoprotein-II inhibitor	–	–	–	–	–	–
Distribution						
VDss (human)	−0.764	−0.268	−0.025	−0.819	−0.252	−0.259
Fraction unbound	0.052	0.149	0.015	0.202	0.158	0.175
BBB permeability	−1.725	0.046	−0.158	−1.165	0.017	0.013
CNS permeability	−4.013	−2.083	−1.483	−2.876	−2.208	−2.286
Metabolism						
CYP2D6 substrate	–	–	–	–	–	–
CYP3A4 substrate	+	+	+	–	+	+
CYP1A2 inhibitor	–	–	–	–	–	–
CYP2C19 inhibitor	–	–	–	–	–	–
CYP2C9 inhibitor	–	–	–	–	–	–
CYP2D6 inhibitor	–	–	–	–	–	–
CYP3A4 inhibitor	+	–	–	–	–	–
Excretion						
Total clearance	0.713	1.19	1.115	0.952	1.175	1.301
Renal OCT2 substrate	–	+	–	–	+	+
Toxicity						
AMES toxicity	–	–	–	–	–	–
Maximum tolerated dose	0.015	−0.124	−0.616	−0.953	−0.127	−0.127
hERG I inhibitor	–	–	–	–	–	–
hERG II inhibitor	+	–	–	–	–	–
Oral rate acute toxicity (LD50)	4.138	3.433	2.678	4.065	2.655	2.622
Oral rat chronic toxicity (LOAEL)	3.606	1.57	2.056	3.566	1.567	1.487
Hepatotoxicity	+	–	–	–	–	–
Skin sensitization	–	–	–	–	–	–
T. pyriformis toxicity	0.285	0.443	0.865	0.285	0.447	0.441
Minnow toxicity	4.885	0.484	−0.723	5.135	0.443	0.537

Table 4
Molecular docking results with maximum binding affinity of selected bioactive compounds from *A. panniculata* against M^{pro} COVID-19 (6LU7) and its cellular receptor.

Ligands	Molecular formula	Molecular weight	No of H- bond	H-bond distance Å	Binding energy (Kcal/mol)	Inhibition constant (Ki) μM	Interacting amino acid residues
N3	$C_{35}H_{48}N_6O_8$	680.00	4	1.56, 2.50, 3.07, 2.58	−7.69	2.32	Gly143, Ser144, His164, Glu166
Andrographolide	$C_{20}H_{30}O_5$	332.00	2	2.07, 1.90	−8.09	1.18	Phe140, Ser144
Andrograpanin	$C_{20}H_{30}O_3$	318.00	2	2.94, 2.13	−7.62	2.59	His41, Asn142
Neoandrographolide	$C_{26}H_{40}O_8$	480.00	6	2.62, 2.74, 2.17, 1.96, 2.07, 2.20	−7.76	2.05	Cys145, Met165, Glu166, Arg188, Gln189
14-Deoxyandrographolide	$C_{20}H_{30}O_4$	334.00	3	2.99, 2.00, 2.17	−7.67	2.40	His41, Leu141
14-deoxy-11,12-didehydroandropholide	$C_{20}H_{28}O_4$	332.00	4	2.82, 2.09, 1.98, 2.25	−7.92	1.57	His41, Tyr54, Leu141, Ser144

drugs against COVID-19 since, they have already evaluated the toxicity and safety in human against the management of different diseases (Kandeel and Al-Nazawi, 2020). The latest discovery of M^{pro} structure of COVID-19 offers a promising possibility of detecting prospective pharma-kinetic candidates in successful COVID therapy. Several of antiviral bioactive compounds have been isolated and used in the pharmaceutical. Natural products have increased significance in this sense in recent decades as effective antiviral agents (Prasanth et al., 2021). The RO5 rule is used for the determination of the drug-like energy and if any bioactive molecule possesses physico-chemical properties to be used as an active drug that can be consumed orally in humans (Lipinski, 2004). In determining whether a molecule has drug-likeness, one of them is to follow RO5. Taking this into account, we have screened five diterpenoids from *A. panniculata* as novel ligand molecules against M^{pro} of COVID-19. The study results demonstrated that the selected all five ligands found to adapt the RO5 without incurring any violation of the RO5, while native ligand N3 incurred two violations. It is also used to predict the probability of success or failure of the molecule with biological activity to be developed as a drug.

We further explored the ADME pharmacokinetics, absorption, distribution, excretion and toxicity of selected bioactive compounds by using Swiss ADME and admetSAR server and the study findings were shown in Table 3. The polar surface area of all the diterpenoids except neoandrographolide was found to be < 100, which implies that the diterpenoids except neoandrographolide

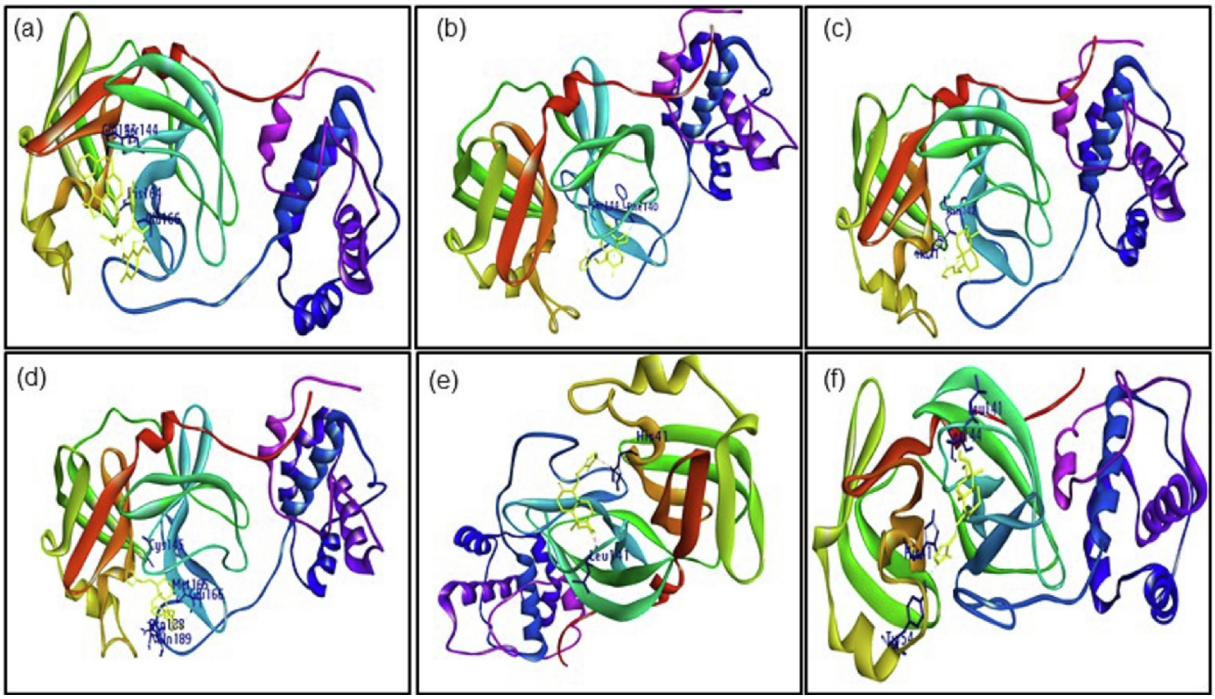

Fig. 1. **(a)** Binding sites for N3 ligands within M^{pro} of COVID-19. **(b)** Binding sites for andrographolide ligands within M^{pro} of COVID-19. **(c)** Binding sites for andrograpanin ligands within M^{pro} of COVID-19. **(d)** Binding sites for neoandrographolide ligands within M^{pro} of COVID-19. **(e)** Binding sites for 14-deoxyandrographolide ligands within M^{pro} of COVID-19. **(f)** Binding sites for 14–11,12-didehydroandrographolide ligands within M^{pro} of COVID-19.

had greater membrane permeability or oral absorption. AlogP values helps in determining the lipophilicity of a compound, if the value of AlogP < 5, then the compound will have good lipophilicity (Han et al., 2019). Taking this into account, we also determined the AlogP value for all selected bioactive compound and the results of the study showed that AlogP value for all compounds were < 5 that indicating these selected compounds have ideal lipophilicity.

Also, in this study, we determined the absorption characteristics of bioactive molecules using $CaCO_2$ permeability, intestinal absorption, skin permeability and P-Glycoprotein substrate or inhibitor. If the Papp Coefficient value is > $8x10^{-6}$ and the predicted value is > 0.90 then the molecule will be easily absorbed. Among the results, all the selected bioactive molecules showed the Papp Coefficient value was > $8x10^{-6}$, this indicates that the selected molecules are easy to absorb due to its high permeability property. Bioactive molecules with intestinal absorption percentage < 30 were considered to have a low intestinal absorption. Since the entire selected bioactive molecules intestinal absorption % value was than < 30, which confirm the good intestinal absorption. Among the selected compounds, andrograpanin had greater intestinal absorption (100%), and neoandrographolide had lower intestinal absorption (499.25%). Same like, our study results also showed the greater Log Kp values for all the selected compounds. P-Glycoprotein is a transporter protein that belongs to the family of ATP-binding cassette (ABC), plays a key function in eliminating Xenobiotics and toxins from the cells (Lin and Yamazaki, 2003). It has two isoforms, class I (drug transport) and class II isoforms (export phosphatidylcholine to bile). Moreover, P-Glycoprotein inhibitors increase the drug bioavailability in the cell by inhibiting P-Glycoprotein. All five diterpenoids were found to act as a substrate for P-Glycoprotein to remove them from the cells, and these selected bioactive molecules were acting as inhibitor for P-Glycoprotein I not for P-Glycoprotein II.

The drug distribution in tissues *in-vitro* and *in-vivo* can be measured by determining the volume of distribution (Vd). The compounds high distribution is considered when value of Log Vs is > 0.45 (Log Vd > 0.45), but our study results showed that all selected bioactive molecules had lower distribution value. The blood brain barrier (BBB) is considered as an important factor to analyse the drug permeability, and this permeability analysis is mainly done to drug used to treat CNS related illness. BBB permeability is measured in terms of LogBBB, if the value > 0.3 then the compounds will have good BBB permeability, if the LogBBB value between 0.3 to −1 then the compound can still pass via BBB and if the value <−1 then the compound relatively have poor BBB permeability (Kunwittaya et al., 2013).

Cytochrome P450 (cyt P450) is a heme-containing enzymes, is located on the lipid bilayer of the endoplasmic reticulum of the hepatocytes and most of drugs, steroids, and carcinogens metabolisms takes place in it with the help of cyt P450 enzyme (Guengerich et al., 2019). CYP2D6 and CYP3A4 are two main subtypes of cyt P450. From the study, we confirmed that the selected compounds except neoandrographolide can be metabolized in liver due to its substrate function. According to AMES study analysis, no toxicity was found for all selected bioactive compounds, since the hERG channel is not affected, there is no cardiotoxicity, and skin sensitization was noted by these biomolecules.

For a successful drug development, it is important that the lead molecule should exhibit maximal potency against the drug target, be safe as well as have appropriate pharmacokinetic properties. Hence, determination of pharmacokinetic properties is important. The pharmacokinetics study of N3 inhibitor showed that the compounds had lower absorption, good lipophilicity, less permeability, greater intestinal absorption and lower skin permeability, N3 act as both substrate and inhibitor for P-glycoprotein I, which implies that the compound can be excreted from the cells and they showed good bioavailability. Also, the result showed that the distribution volume of the compound was very low and the ability to cross BBB and CNS was shown very low, the compound act as both substrate and inhibitor for CYP3A4 which indicates that it can be metabolized in liver. ADMET profiling is critical phase of drug finding and development research as it

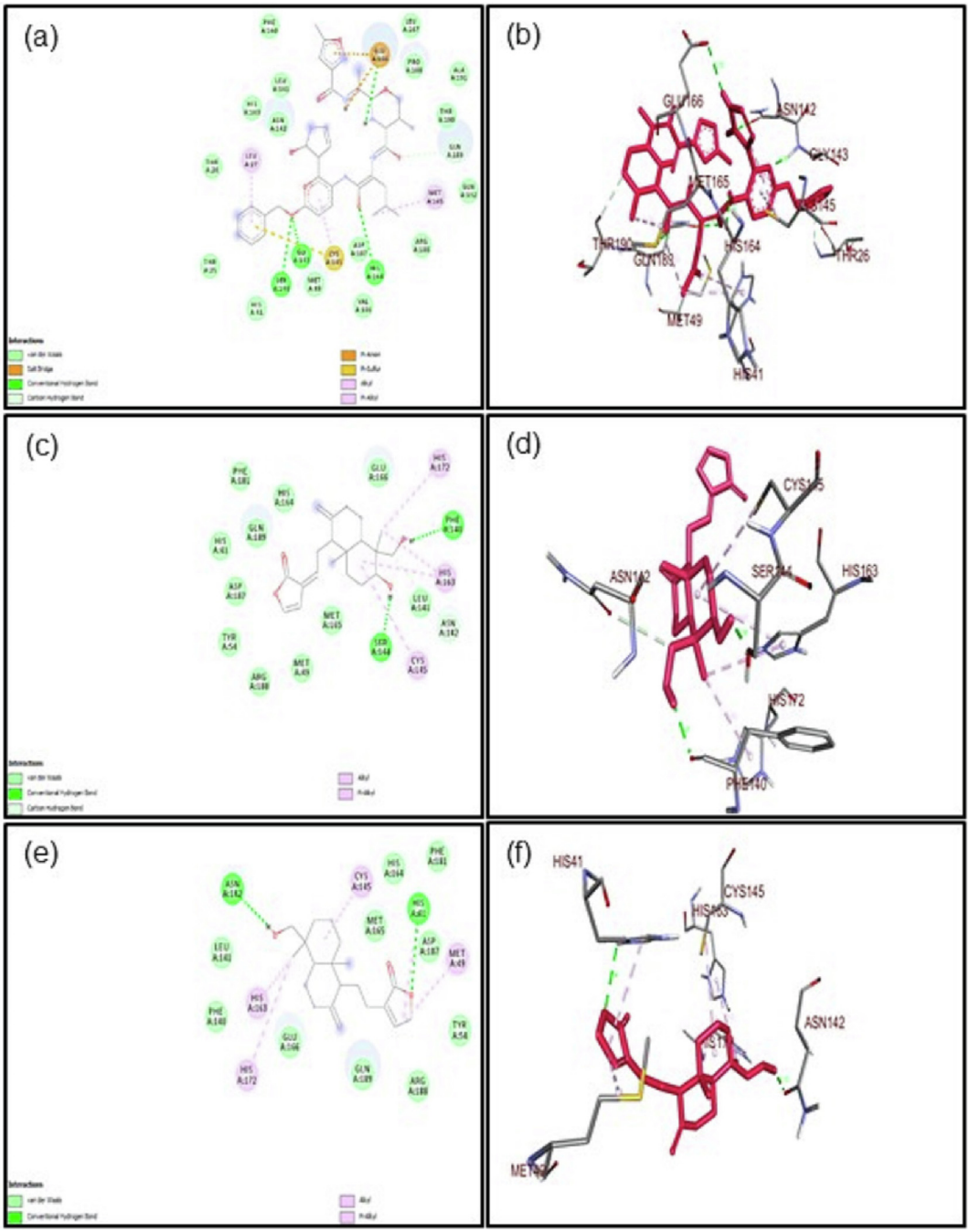

Fig. 2. **(a and b)** 2D and 3D structural interaction view of N3 ligands with M^{pro} of COVID-19. **(c and d)** 2D and 3D structural interaction view of andrographolide ligands with M^{pro} of COVID-19. **(e and f)** 2D and 3D structural interaction view of neoandrographolide ligands with M^{pro} of COVID-19.

helps in obtaining the optimal balance of properties necessary for load or hit discovery that are eventually safe and effective. As stated by ADMET result, N3 was found to be hepatotoxic and cardiotoxic nature.

Concerning a ligand to serve as a therapeutic molecule, it must bind to a specific catalyst site with significant relationship. In some cases, the ligands binds to the allosteric sites, which leads to specific structure or changes to compliance with the binding site modulation or inhibition of molecular binding (Poongavanam et al., 2019). We speculate that in case of M^{pro} COVID-19, even though the ligands are not binding to interfacial regions, they may indirectly affect the binding of M^{pro} to COVID-19 receptor. The study findings clearly showed that andrographolide had a greater affinity to M^{pro} of COVID-19 than native ligand N3 and other selected bioactive compounds.

From the *in-silico* studies, it clearly showed that all selected bioactive compounds had a good binding energy towards the M^{pro} of COVID-19. The binding energy value of −6 Kcal/mol is considered as the upper threshold value for ligand binding study, if the binding energy value is > -6 Kcal/mol then the ligands it is considered it have good binding affinity with receptor. Our study results also revealed that all the selected compounds had a binding energy > -6. But, the binding of the native ligand N3 to the two catalytic residues (His41 and Cys145) were considered the major fac-

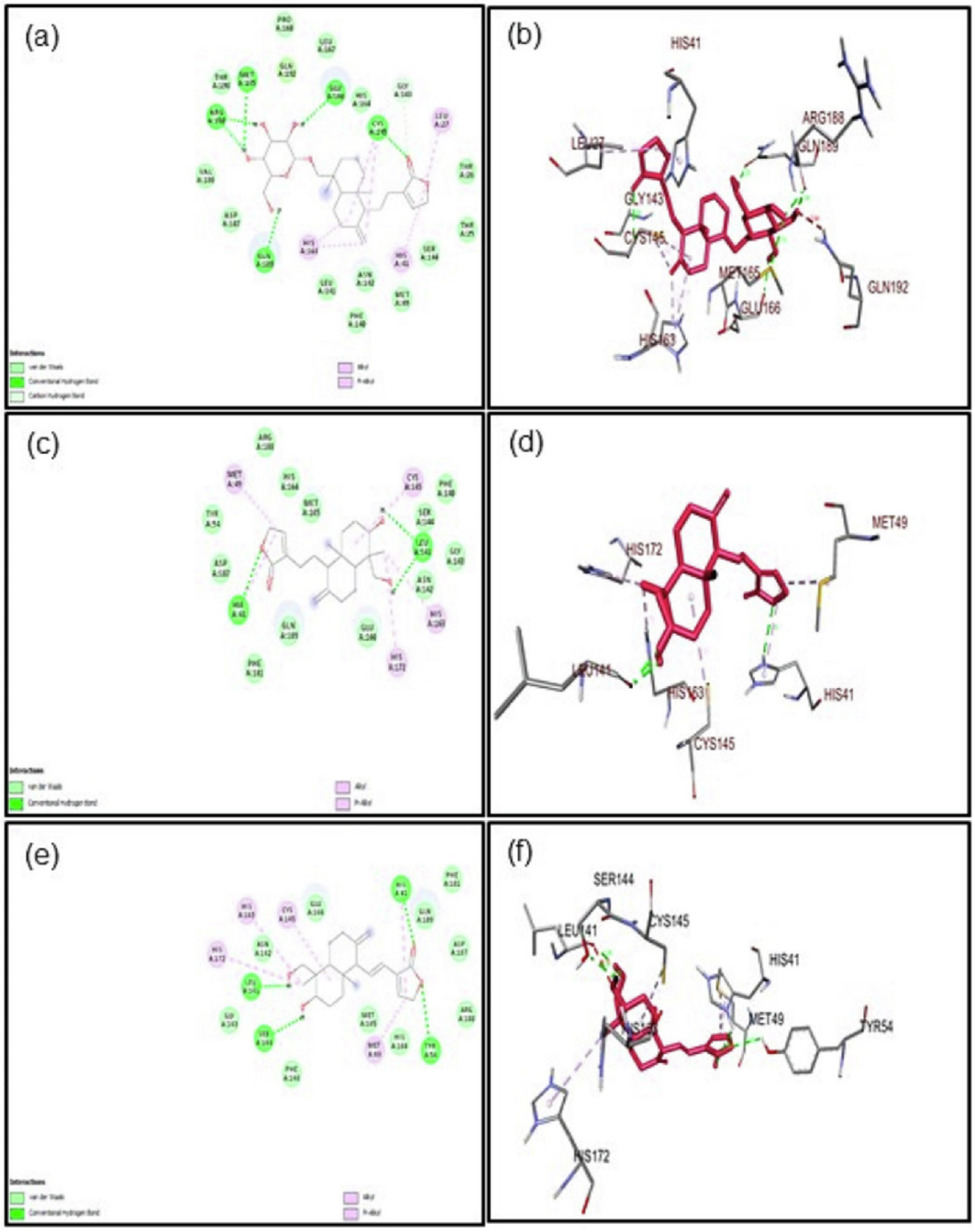

Fig. 3. (a and b) 2D and 3D structural interaction view of andrograpanin ligands with M^{pro} of COVID-19. **(c and d)** 2D and 3D structural interaction view of 14-deoxyandrographolide ligands with M^{pro} of COVID-19. **(e and f)** 2D and 3D structural interaction view of 14–11,12-didehydroandrographolide ligands with M^{pro} of COVID-19.

tor determining the ability of the inhibitor to inhibit the protease activity of the M^{pro} of COVID-19 (Ghosh et al., 2021). Similarly, all of selected bioactive compounds also bind with these two catalytic residues (His41 and Cys145) when both the hydrogen and non-hydrogen bonds were considered. In addition, it has been found that the andrographolide have better binding energy towards M^{pro} of COVID-19 compared with other bioactive compounds due to their ability of binding affinity with two catalytic residues (His41 and Cys145). Apart from andrographolide other selected bioactive compounds have also demonstrated a significant binding energy towards M^{pro} of COVID-19. When the inhibition constant Ki values of the selected bioactive compounds are taken into account, andrographolide has the lowest Ki value, which represents the ability to inhibit the M^{pro} of COVID-19 at low concentration. Earlier literature also demonstrated the antiviral activity of andrographolide against HIV, HSV and EBV viruses (Jayakumar et al., 2013).

To investigate the protein stability and atom movements during the molecular association, molecular dynamics and simulation are playing significant role in the post docking studies. Main protease with andrographolide derivatives were analyzed for conformational changes and constraints. Trajectories recorded for 50 nano seconds were chosen to evaluate the ligand position during a longer simulation by root mean square deviation, fluctuation

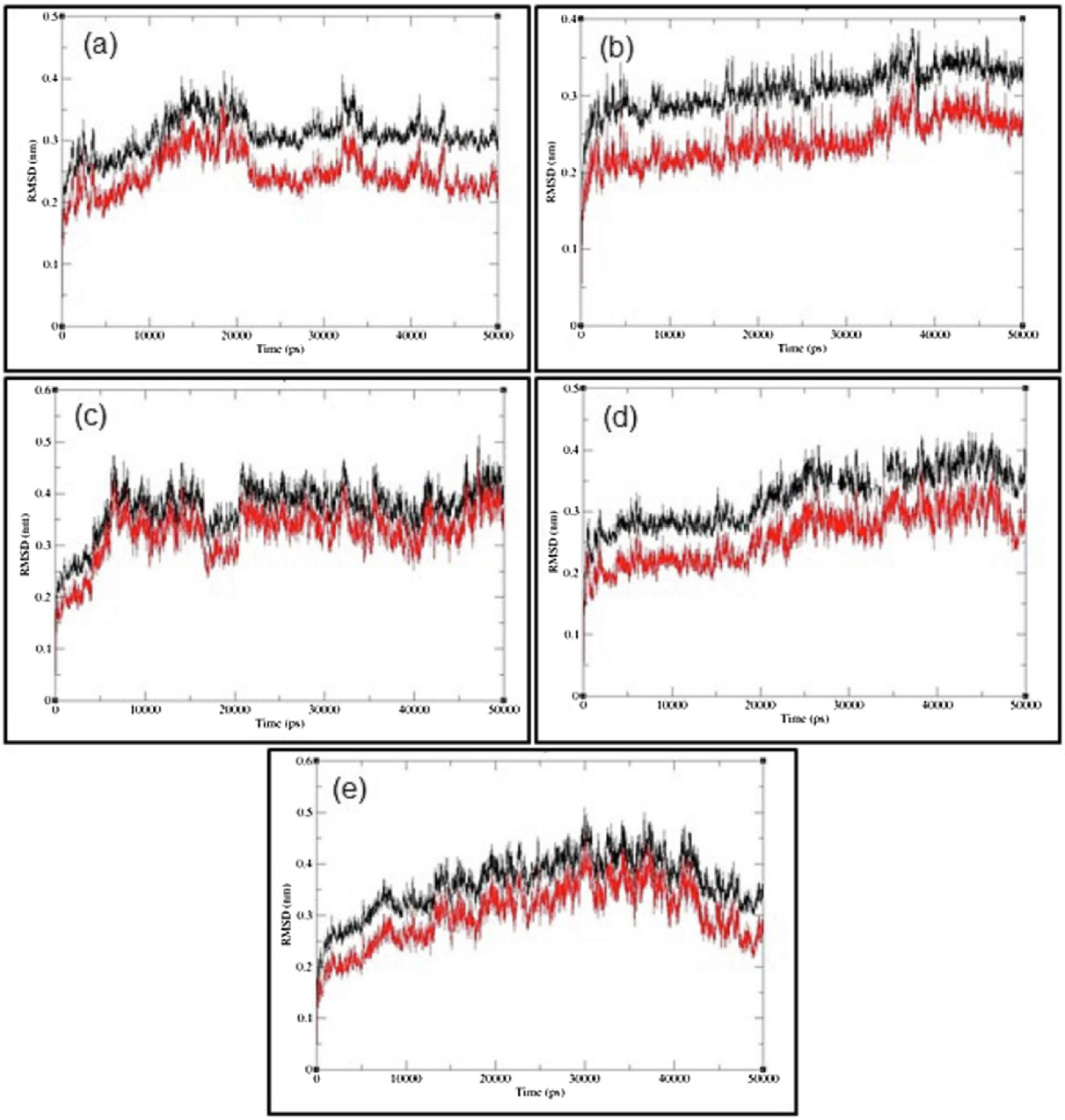

Fig. 4. The RMSD plots, **(a)** andrographolide, **(b)** andrographonin, **(c)** neoandrographolide, **(d)** 14-deoxyandrographolide, **(e)** 14-deoxy-11,12-didehydroandropholide, are clearly indicating the back bone and ligand fit following the stability curve and the ligands found constantly (block line: protein C-α and red line: ligand rmsd).

and hydrogen bonding. From the result of RMSD (Fig. 4), RMSF (Fig. 5) and hydrogen bonding plots (Fig. 6), it is observed that main protease – andrographolide derivatives are strong enough to maintain stability. Differences in RMSD were observed for the diterpenoids, which is under 0.5 (nm), respectively. Hydrogen bonding is mainly considered for stability and interaction of system, which makes the rigidity between main protease- inhibitors. RMSF plot explains the residues fluctuating among 306 amino acids as confirmation change over time period. Consequently, N and C terminal residues have undergone high fluctuation. Combined result of ligand bound RMSD showing that the first 5 ns are constant for all the main protease-inhibitors. Next 45 nano seconds, ligand bound state moved vigorously were revealed by comparing root mean square deviation. Energies obtained in docking process were then tabulated to distinguish the Free energy of binding, Vander Waals, electrostatic, inter molecular, torsional energies and unbound system. Free energy of binding and Vander Waals energies were high for andrographolide as −0.76 kcal/mol and −8.49 kcal/mol, while electrostatic energy is −0.06 kcal/mol. In order to compare the free energy of binding, bar plot was presented that shows the slight difference among diterpenoids. All the diterpenoids differed in physicochemical properties were sharing the free energy of binding between −5 to −8 kcal/mol. In total, binding energies have been calculated and considered for better interaction that are reasonable for andrographolide (-7.06 kcal/mol) and 14-deoxyandrographolide (-7.01 kcal/mol). 14-deoxy-11,12-didehydroandropholide (-6.96 kcal/mol) and andrographonin (-6.87 kcal/mol) are recorded for energy differences while neoandrographolide is found with −5.47 kcal/mol.

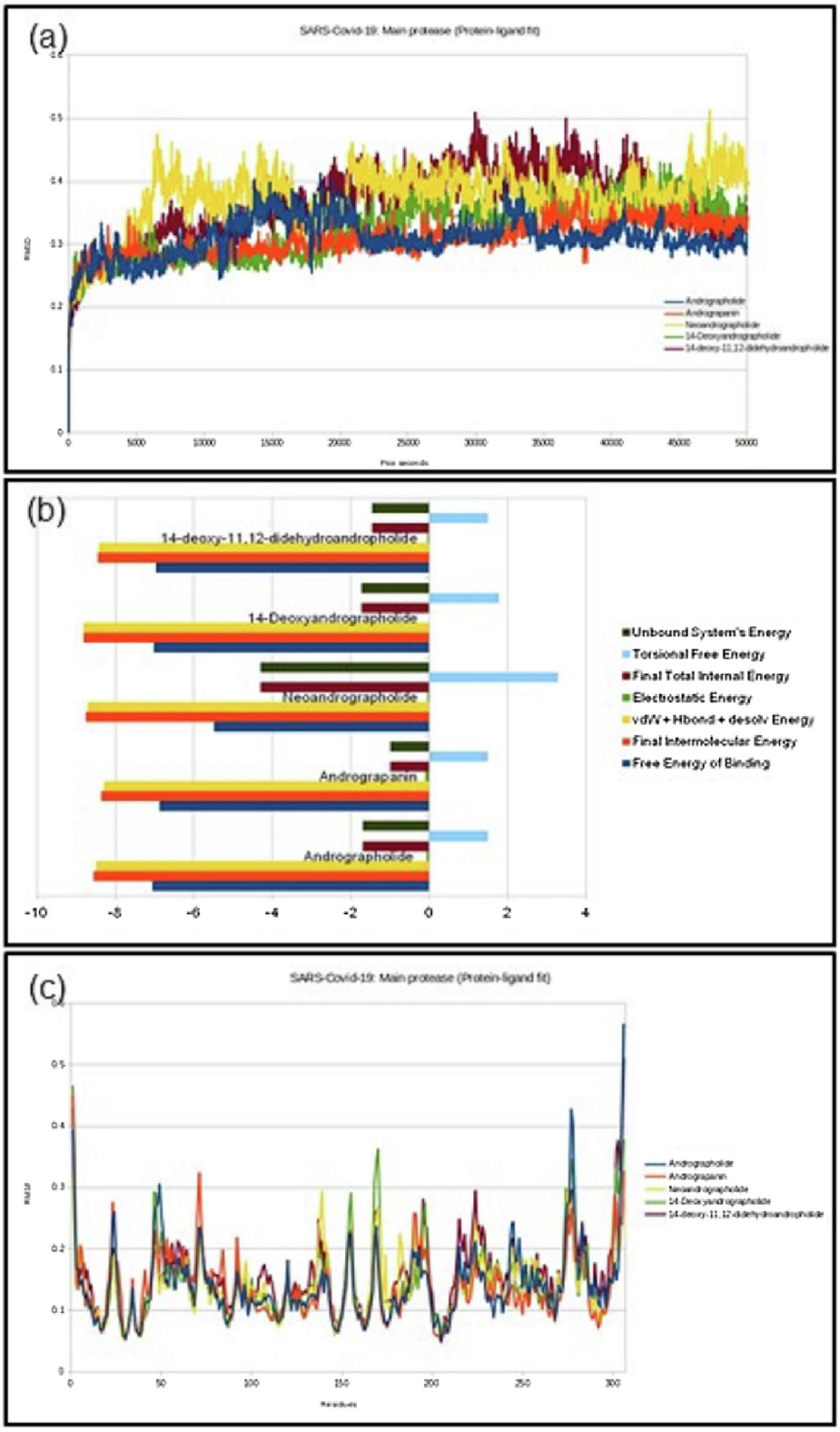

Fig. 5. **(a)** Ligand fit RMSD comparison among diterpenoids exhibits atomic details of aberration. **(b)** Predicted free energy of binding of diterpenoids reveals the interaction energy. **(c)** XY-scatter diagram of root mean square fluctuation indicating the amino acids fluctuation with residue number.

5. Conclusion

Together, based on our knowledge this is the first report proven the efficacy of the selected five diterpenoids compounds from *A. panniculata* against crystal structure of SARS-CoV-2 M^{pro} (6LU7). Among the study findings, all diterpenoids, especially andrographolide can effectively inhibit the interaction between M^{pro} of SARS-CoV-2 with its receptor. Also the pharmacokinetic and

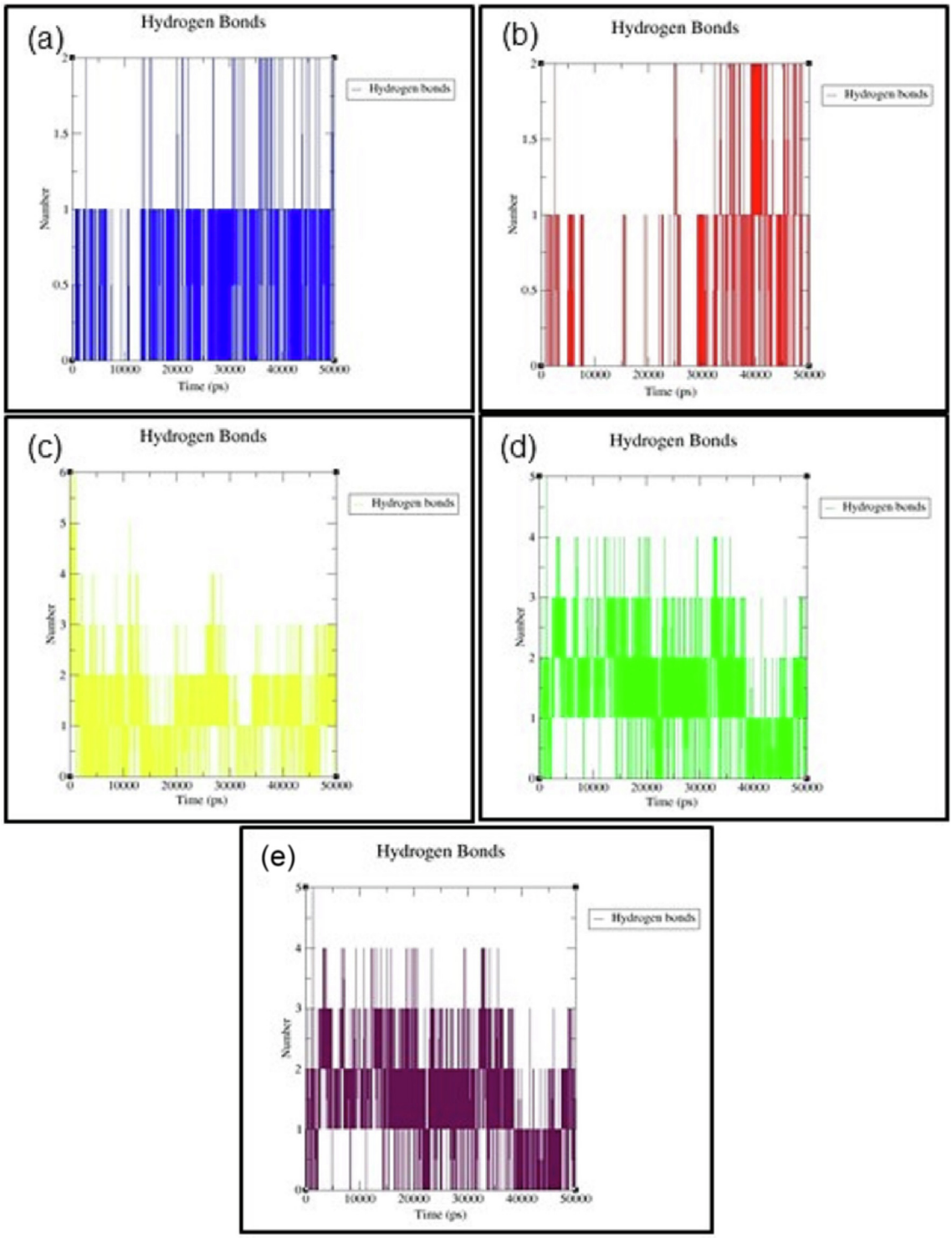

Fig. 6. The hydrogen bond plots, **(a)** andrographolide, **(b)** andrographonin, **(c)** neoandrographolide, **(d)** 14-deoxyandrographolide, **(e)** 14-deoxy-11,12-didehydroandrophlide, are dictating the movements and number of hydrogen bonds with 50,000 picoseconds (ps).

molecular dynamic simulation study results proved that all selected diterpenoids compounds from *A. panniculata* have good pharmacological properties such as no violation, better absorption property, bioavailability, BBB permeability, low toxicity and inhibition constant Ki value. Hence, according to our study findings, it is suggested that andrographolide from *A. panniculata* can be useful therapeutic molecule against SARS-CoV-2 for controlling viral attachment to the host cells through the inhibition of M^{pro} of SARS-CoV-2. However, further study is warranted to validate the therapeutic ability of andrographolide in *in-vivo* model.

Declaration of Competing Interest

The authors declare that they have no known competing financial interests or personal relationships that could have appeared to influence the work reported in this paper.

Acknowledgements

We acknowledge the Management, Principal and Secretary of PSG College of Arts & Science, Coimbatore, Tamil Nadu, India for their continuous support to carry out this research.

References

Ahmed, W., Angel, N., Edson, J., Bibby, K., Bivins, A., O'Brien, J.W., Choi, P.M., Kitajima, M., Simpson, S.L., Li, J., Tscharke, B., Verhagen, R., Smith, W.J.M., Zaugg, J., Dierens, L., Hugenholtz, P., Thomas, K.V., Mueller, J.F., 2020. First confirmed detection of SARS-CoV-2 in untreated wastewater in Australia: A proof of concept for the wastewater surveillance of COVID-19 in the community. Sci. Total Environ. 728, 138764. https://doi.org/10.1016/j.scitotenv.2020.138764.

Arasu, A., Balakrishnan, P., Velusamy, T., Ramesh, T., 2020. Can Mandated BCG Vaccine Promote herd Immunity against Novel Coronavirus? A Potential Solution at Hand to Tackle Covid-19 Pandemic. Curr. Immunol. Rev. 16 (1), 6–11.

Bhojaraj, S., Ananda Kumar, T., Ghosh, A., Sushmitha, B.S., Ramamurthy, S., Velusamy, T., Ramesh, T., Jayanthi, M.K., Essa, M., Chidambaram, S., Qoronfleh, M.W., 2021. Biosimilars: An Update. Int. J. Nutr. Pharmacol. Neurol. Dis. 11 (1), 7. https://doi.org/10.4103/ijnpnd.ijnpnd_96_20.

Chao, W.-W., Lin, B.-F., 2010. Isolation and identification of bioactive compounds in Andrographis paniculata (Chuanxinlian). Chin. Med. 5 (1), 17. https://doi.org/10.1186/1749-8546-5-17.

Cui, J., Li, F., Shi, Z.-L., 2019. Origin and evolution of pathogenic coronaviruses. Nat. Rev. Microbiol. 17 (3), 181–192.

Denaro, M., Smeriglio, A., Barreca, D., De Francesco, C., Occhiuto, C., Milano, G., Trombetta, D., 2020. Antiviral activity of plants and their isolated bioactive compounds: An update. Phytother. Res. 34 (4), 742–768.

Ghosh, R., Chakraborty, A., Biswas, A., Chowdhuri, S., 2021. Evaluation of green tea polyphenols as novel corona virus (SARS CoV-2) main protease (Mpro) inhibitors - an in silico docking and molecular dynamics simulation study. J. Biomol. Struct. Dyn. 39 (12), 4362–4374.

Gil, C., Ginex, T., Maestro, I., Nozal, V., Barrado-Gil, L., Cuesta-Geijo, M.Á., Urquiza, J., Ramírez, D., Alonso, C., Campillo, N.E., Martinez, A., 2020. COVID-19: Drug Targets and Potential Treatments. J. Med. Chem. 63 (21), 12359–12386.

Guengerich, F.P., Wilkey, C.J., Phan, T.T.N., 2019. Human cytochrome P450 enzymes bind drugs and other substrates mainly through conformational-selection modes. J. Biol. Chem. 294 (28), 10928–10941.

Han, Y., Zhang, J., Hu, C.Q., Zhang, X., Ma, B., Zhang, P., 2019. In silico ADME and Toxicity Prediction of Ceftazidime and Its Impurities. Front. Pharmacol. 10, 434.

Hussain, W., Haleem, K.S., Khan, I., Tauseef, I., Qayyum, S., Ahmed, B., Riaz, M.N., 2017. Medicinal plants: a repository of antiviral metabolites. Future Virol. 12 (6), 299–308.

Jayakumar, T., Hsieh, C.-Y., Lee, J.-J., Sheu, J.-R., 2013. Experimental and Clinical Pharmacology of Andrographis paniculata and Its Major Bioactive Phytoconstituent Andrographolide. Evid. Based Complement. Alternat. Med. 2013, 1–16.

Kandeel, M., Al-Nazawi, M., 2020. Virtual screening and repurposing of FDA approved drugs against COVID-19 main protease. Life Sci. 251, 117627. https://doi.org/10.1016/j.lfs.2020.117627.

Kumar, D., Kumari, K., Vishvakarma, V.K., Jayaraj, A., Kumar, D., Ramappa, V.K., Patel, R., Kumar, V., Dass, S.K., Chandra, R., Singh, P., 2021. Promising inhibitors of main protease of novel corona virus to prevent the spread of COVID-19 using docking and molecular dynamics simulation. J. Biomol. Struct. Dyn. 39 (13), 4671–4685.

Kumar, D., Manuel, O., Natori, Y., Egawa, H., Grossi, P., Han, S.-H., Fernández-Ruiz, M., Humar, A., 2020. COVID-19: A global transplant perspective on successfully navigating a pandemic. Am. J. Transplant. 20 (7), 1773–1779.

Kunwittaya, S., Nantasenamat, C., Treeratanapiboon, L., Srisarin, A., Isarankura-Na-Ayudhya, C., Prachayasittikul, V., 2013. Influence of logBB cut-off on the prediction of blood-brain barrier permeability. Biomed. App. Technol. J. 1, 16–34.

Lee, S.Y., Hur, S.J., 2017. Antihypertensive peptides from animal products, marine organisms, and plants. Food Chem. 228, 506–517.

Lin, J.H., Yamazaki, M., 2003. Clinical relevance of P-glycoprotein in drug therapy. Drug Metab. Rev. 35 (4), 417–454.

Lin, L.-T., Hsu, W.-C., Lin, C.-C., 2014. Antiviral natural products and herbal medicines. J. Tradit. Complement Med. 4 (1), 24–35.

Lipinski, C.A., 2004. Lead- and drug-like compounds: the rule-of-five revolution. Drug Discov. Today Technol. 1 (4), 337–341.

Liu, P.P., Blet, A., Smyth, D., Li, H., 2020. The Science Underlying COVID-19: Implications for the Cardiovascular System. Circulation 142 (1), 68–78.

Mishra, U.S., Mishra, A., Kumari, R., Murthy, P.N., Naik, B.S., 2009. Antibacterial Activity of Ethanol Extract of Andrographis paniculata. Indian J. Pharm. Sci. 71 (4), 436–438.

Okhuarobo, A., Ehizogie Falodun, J., Erharuyi, O., Imieje, V., Falodun, A., Langer, P., 2014. Harnessing the medicinal properties of Andrographis paniculata for diseases and beyond: a review of its phytochemistry and pharmacology. Asian Pac. J. Trop. Dis. 4 (3), 213–222.

Poongavanam, V., Kongsted, J., Wüstner, D., 2019. Computational Modeling Explains the Multi Sterol Ligand Specificity of the N-Terminal Domain of Niemann-Pick C1-Like 1 Protein. ACS Omega. 4 (25), 20894–20904.

Prasanth, D.S.N.B.K., Murahari, M., Chandramohan, V., Panda, S.P., Atmakuri, L.R., Guntupalli, C., 2021. In silico identification of potential inhibitors from Cinnamon against main protease and spike glycoprotein of SARS CoV-2. J. Biomol. Struct. Dyn. 39 (13), 4618–4632.

Rosidi, A., Khomsan, A., Setiawan, B., Riyadi, H., Briawan, D., 2016. Antioxidant Potential of Temulawak (Curcuma xanthorrhiza roxb). Pak. J. Nutr. 15 (6), 556–560.

Salehi, S., Abedi, A., Balakrishnan, S., Gholamrezanezhad, A., 2020. Coronavirus Disease 2019 (COVID-19): A Systematic Review of Imaging Findings in 919 Patients. Am. J. Roentgenol. 215 (1), 87–93.

Sheikh, A., Al-Taher, A., Al-Nazawi, M., Al-Mubarak, A.I., Kandeel, M., 2020. Analysis of preferred codon usage in the coronavirus N genes and their implications for genome evolution and vaccine design. J. Virol. Methods. 277, 113806. https://doi.org/10.1016/j.jviromet.2019.113806.

Shetty, R., Ghosh, A., Honavar, S.G., Khamar, P., Sethu, S., 2020. Therapeutic opportunities to manage COVID-19/SARS-CoV-2 infection: Present and future. Indian J. Ophthalmol. 68 (5), 693–702.

Wahedi, H.M., Ahmad, S., Abbasi, S.W., 2021. Stilbene-based natural compounds as promising drug candidates against COVID-19. J. Biomol. Struct. Dyn. 39 (9), 3225–3234.

Wang, D., Hu, B., Hu, C., Zhu, F., Liu, X., Zhang, J., Wang, B., Xiang, H., Cheng, Z., Xiong, Y., Zhao, Y., Li, Y., Wang, X., Peng, Z., 2020. Clinical Characteristics of 138 Hospitalized Patients With 2019 Novel Coronavirus-Infected Pneumonia in Wuhan. China. JAMA. 323 (11), 1061–1069.